Fault Location for the NEPTUNE Power System

Ting Chan, *Student Member, IEEE*, Chen-Ching Liu, *Fellow, IEEE*, Bruce M. Howe, *Member, IEEE*, and Harold Kirkham, *Fellow, IEEE*

***Abstract*—The objective of the North Eastern Pacific Time-Series Undersea Networked Experiment (NEPTUNE) program is to construct an underwater cabled observatory on the floor of the Pacific Ocean, encompassing the Juan de Fuca Tectonic Plate. The power system associated with the proposed observatory is unlike conventional terrestrial power systems in many ways due to the unique operating conditions of underwater cabled observatories. In the event of a backbone cable fault, the location of the fault must be identified accurately so that a repair ship can be sent to repair the cable. Due to the proposed networked, mesh structure, traditional techniques for cable fault identification can not achieve the desired level of accuracy. In this paper, a system-theoretic method is proposed for identification of the fault location based on the limited data available. The method has been tested with extensive simulations and is being implemented for the field test in Monterey, California. In this study, a lab test is performed for the fault location function.**

***Index Terms*—Current measurement, DC power systems, fault location, underwater technology, voltage measurement.**

I. Introduction

THE STUDY of the undersea environment requires the use of scientific instrumentation. This instrumentation has typically used batteries for its electrical power requirements. This severe limitation restricts the duration as well as the efficiency with which the studies are conducted. The North Eastern Pacific Time-Series Undersea Networked Experiment (NEPTUNE) system will provide an underwater cabled network in the Pacific Ocean so that continuous electrical power can be supplied to science users [1]–[5].

Traditional terrestrial power systems are normally AC networked parallel configurations while underwater telecommunication systems are normally DC series cabled systems. The proposed NEPTUNE power system differs from both of them in that the NEPTUNE power system is a DC networked system. It is planned to have approximately 3000 km of cables with two shore stations (Victoria and Nedonna Beach) and up to 46 science nodes, as illustrated in Fig. 1. At each of the shore stations, a -10 kV DC power supply will be used to provide power that serves the entire system. At each of the science nodes, a DC-DC power converter is used to convert the voltage level down to 400 and 48 V for science users.

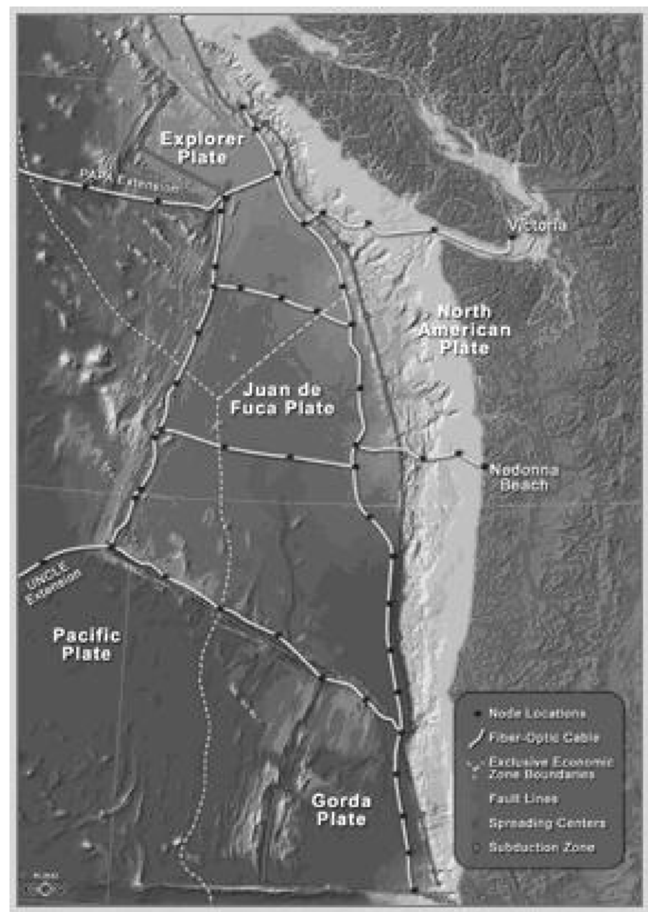

Fig. 1. NEPTUNE system.

The cable connecting the science nodes is called the backbone. At each of the node locations, a branching unit (BU) is used to connect the backbone cable with the science node through a spur cable. The connection with the backbone cable, BU, and the science node is shown in Fig. 2. In case of a backbone or spur cable fault, switches in the BU will be opened to isolate the fault so that the rest of the system will remain in operation. The power supply for the switches inside the BU is based on Zener diodes. The BU control system does not require communications from the shore stations or science nodes [6]. In the current design, the length of the backbone cable between each of the BUs ranges from tens of kilometers to over 100 km. The lengths of spur cables would be several to tens of kilometers.

The repair/replacement cost of a component for an underwater observatory system can be very high. Therefore, a crucial

Manuscript received February 28, 2006; revised September 15, 2006. This work was supported by the National Science Foundation through grant OCE-0116750, "Development of a power system for cabled ocean Observatories." Paper no. TPWRS-00106-2006.

T. Chan is with the Department of Electrical Engineering, University of Washington, Seattle, WA 98195-2500 USA (e-mail: tingc@u.washington.edu).

C.-C. Liu is with the Department of Electrical and Computer Engineering, Iowa State University, Ames, IA 50011 USA (e-mail: liu@iastate.edu).

B. M. Howe is with the Applied Physics Laboratory, University of Washington, Seattle, WA 98195-2500 USA (e-mail: howe@apl.washington.edu).

H. Kirkham is with the Jet Propulsion Laboratory, California Institute of Technology, Pasadena, CA 91109 USA (e-mail: Harold.Kirkham@jpl.nasa.gov).

Color versions of one or more of the figures in this paper are available online at http://ieeexplore.ieee.org.

Digital Object Identifier 10.1109/TPWRS.2007.894855

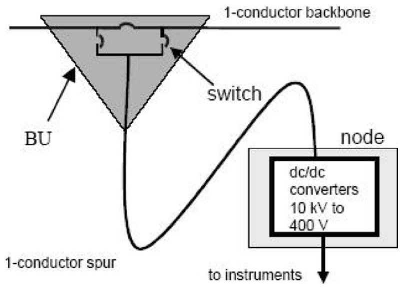

Fig. 2. Connection from backbone cable to a science node through a BU.

design criterion for the NEPTUNE system is a very high level of reliability. The NEPTUNE system has to provide reliable power and communications to the science nodes for a life span of 30 years [3]. It is also our goal to design and implement the system so that minimum maintenance is required over the life span.

One of the main challenges of the NEPTUNE power system is to identify the location of a backbone cable fault. Because limited resources are available to develop a communications system of adequate reliability, it was decided that no communication would be available from shore stations to branching units. As a result, voltages and currents on the backbone and the status of BU switches are not known to the operation center at the shore stations. Unlike traditional power systems, no instantaneous fault data will be available since no recording devices are available on the backbone cable.

II. Power Monitoring and Control System

To locate a fault in a conventional power system, one relies on data collected by recording devices such as digital fault recorders or digital relays at the substations. The data can usually be acquired through the control center of a power company. The control center is also equipped with the Supervisory Control and Data Acquisition System (SCADA) system and Energy Management System (EMS) that provide computer, communication and software facilities for system operators to monitor and control the system.

NEPTUNE's equivalent of a SCADA/EMS is called the Power Monitoring and Control System (PMACS), which consists of the computer software and hardware that controls and monitors the NEPTUNE Power System in a real-time environment. PMACS is constructed with a 3-layer client-server architecture as shown in Fig. 3. The first layer has the Node Power Controller (NPC) and shore Power Supply Controller (PSC) that interact with the hardware in the nodes and shore stations. The middle layer is the PMACS Server, which is responsible for collecting the power system data from science nodes and shore stations, as well as issuing control actions received from the PMACS console; it is the centralized brain of the system. The third layer is the PMACS Console and Client that communicate with the server to gather system parameters such as shore station power supply status, external and internal load status, current and voltage measurements at each bus, converter status, and engineering sensor measurements. The PMACS Console displays the system data and is used to perform control actions, such as turning ON/OFF a specific load, through the user interfaces.

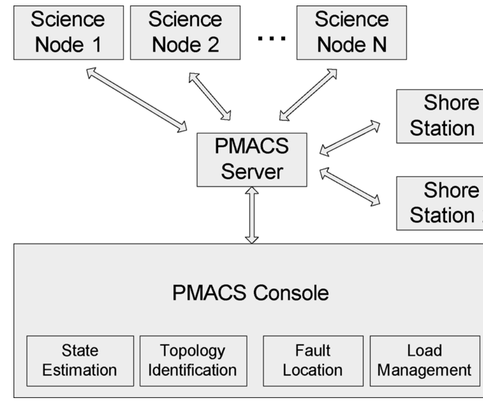

Fig. 3. Power monitoring and control system structure.

PMACS integrates a number of system analysis tools, such as Topology Identification [7], State Estimation [8], Fault Location, and Load Management. In the design of NEPTUNE, a single backbone cable fault would not cause a loss of any science node in most locations after the fault is isolated. However, in case a link is missing, the total power that can be delivered to science nodes can be affected depending on the fault location. Therefore, the faulted cable has to be repaired in order to allow the system to operate at full load. In case of a backbone cable fault, a repair ship is sent to the estimated location of the fault. Deep sea repairs can be slow and costly; therefore, the Fault Location module of PMACS is intended to locate a backbone cable fault to within ± 1 km.

For the NEPTUNE power system, a backbone cable fault causes the entire system to shut down because of voltage collapse. The system then restarts with the shore station voltage at a low positive voltage, $+500$ V. During this time, all switches in the BU will close onto the fault. Since the DC/DC converters at the science nodes require an operating voltage < -5.2 kV, none of the converters will be turned on at the low-voltage level of $+500$ V and, as a result, there is no load or communication in the system. The only circuit carrying currents consists of the backbone cable and the fault in the system. Voltage and current measurements are taken at both shore stations. These measurements will be used by PMACS to determine the fault location. After PMACS takes all the measurements, the polarity at the shore power supply will be reversed (-500 V), a sequence that causes the backbone switches to open and isolate the fault. Service to all loads at the science nodes is then restored [6] by applying the full -10 kV.

Traditional power system fault location techniques involve the use of different protection or recording devices, such as Digital Fault Recorders [9], Digital Relays [10], Sequence of Events Recorders [11], and Phasor Measurement Units [12]. Fault locating methods are normally based on transients in voltages and currents measured by these devices. The usage of these types of devices is not feasible for NEPTUNE due to the physical size limitation of branching units and science nodes.

A common method for identifying submarine cable faults is Time-Domain Reflectometry (TDR) [13]. The same method is used in underground distribution systems [14]. These applications are used for cable lengths from hundreds of meters to tens of kilometers. Faults on the NEPTUNE power system can be situated 1000 km from the shore. If TDR is used, the reflected

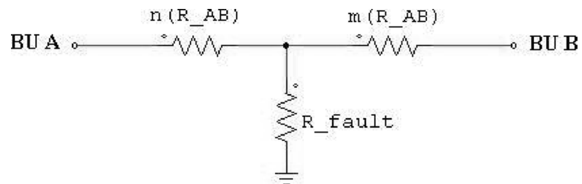

Fig. 4. Fault model.

signal from the fault would be very weak. Furthermore, the branching unit switches and Zener diodes will also generate a large number of reflected signals which further complicate the process of distinguishing the signal from the noise. Hence, it is determined that TDR is impractical for NEPTUNE due to the attenuation and network configuration of the cable system.

For typical submarine cables, fault location can be conducted by applying voltage and current at one end of the cable into the fault and estimating the resistance of the cable. This method would not work for the NEPTUNE system since it is a networked configuration.

In this research, a new fault location algorithm is derived and implemented for a networked DC power system with low observability. The proposed algorithm makes use of the voltage and current measurements taken at the shore stations.

III. Fault Location

In the fault location mode, all switches will be closed and the fault point is drawing all the current, i.e., there are no other loads. Since communication is not available, the only accessible operating conditions are the voltage and current outputs at the shore stations. PMACS uses these measurements to estimate the total cable resistance and the distances between shore stations and the fault.

To locate a backbone cable fault, several additional factors need to be taken into account: 1) the fault characteristics; 2) fault resistance; 3) topology of the system; 4) cable resistance; 5) voltage drop along the cable; and 6) measurement errors.

A. Fault Modeling

A shunt fault on a submarine cable occurs when the cable's insulation deteriorates, allowing sea water to contact the conductor. Typical causes of shunt faults include the following.

- Cable is abraded or partially cut. This can occur if the cable is dragged along the sea floor by a ship's anchor, fishing gear or ocean currents and it sustains cuts and abrasion on the rocky seafloor or outcrops.
- Cable has a manufacturing flaw such as a void or an inclusion in the insulation. If the field at that point is high enough, dielectric breakdown can occur.

In most cases, the cable remains a single piece connecting to the ground with some resistance, instead of completely breaking into two separate pieces [15]. The fault on a given link between two BUs can therefore be modeled by the configuration in Fig. 4.

In Fig. 4, $\mathrm{R\_AB}$ is the resistance of the cable link between branching units A and B. $\mathrm{R\_fault}$ is the *unknown* fault resistance, and n and m are the *unknown* fractional distances from each of the BUs to the fault location, i.e., $n+m=1$.

The fault resistance can vary over a range from a few ohms to tens of ohms depending on the condition of the damaged cable

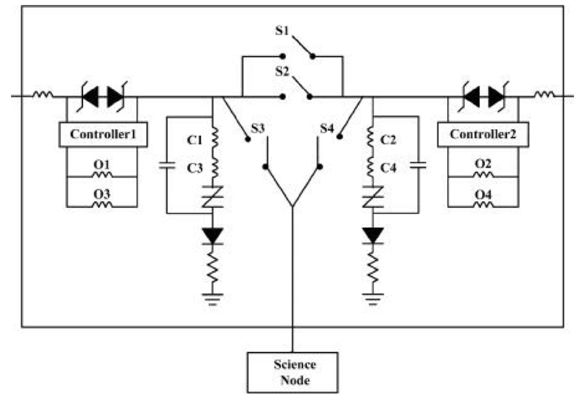

Fig. 5. Branching unit [6].

and how much conductor is exposed to sea water. This range is based on the findings and experience over years by the author of [15] using a fall-of-potential test. The explanation of the fall-of-potential test is included in the Appendix.

B. Component Modeling

It is known that the nominal resistance of the cable is 1 Ω/km or 1.6 Ω/km depending on which of the two types of cable is adopted. However, depending on the actual temperature of the sea water, it could be a few percent lower or higher. There is a temperature coefficient associated with the cable that can be used to calculate the actual resistance based on the temperature of the water (which will likely be available from independent measurements). The estimation of cable resistance can also be done by State Estimation [8].

Besides the cable resistance, constant voltage drops along each section of the cable need to be considered while locating the fault. Across each repeater on the cable, there is a voltage drop. Since a BU includes series Zener diodes, as shown in Fig. 5, there is also a constant voltage drop across each BU. Assuming a BU as shown in Fig. 5, the voltage drop across the BU is calculated as in (1)

$$V_{\mathrm{BU}} = 2 \times V_{Zener\mathrm{Reverse}} + 2 \times V_{ZenerForward}. \quad (1)$$

The Zener reverse bias voltage is 6.9 V, and the forward bias voltage is 0.7 V. Therefore, the voltage drop across one BU circuit is 15.2 V. The voltage drop across a repeater is 7.6 V. The total voltage drop for each section of the backbone is the sum of the repeater voltage drop and the BU voltage drop. The BU design is developed in [6].

C. System Modeling

As mentioned, the minimum operating voltage for the DC/DC converters in the science nodes is 5.2 kV; therefore, there is no load in the system during fault location except the fault itself. Since all switches will be closed onto the fault, the topology of the entire system is known when taking the measurements. The fault is not isolated until all measurements are taken.

Since the system is a meshed network, currents converge to the fault point through multiple paths. Since the system topology is known, the equations for each path can be written taking into account the unknown currents, and known cable resistances and

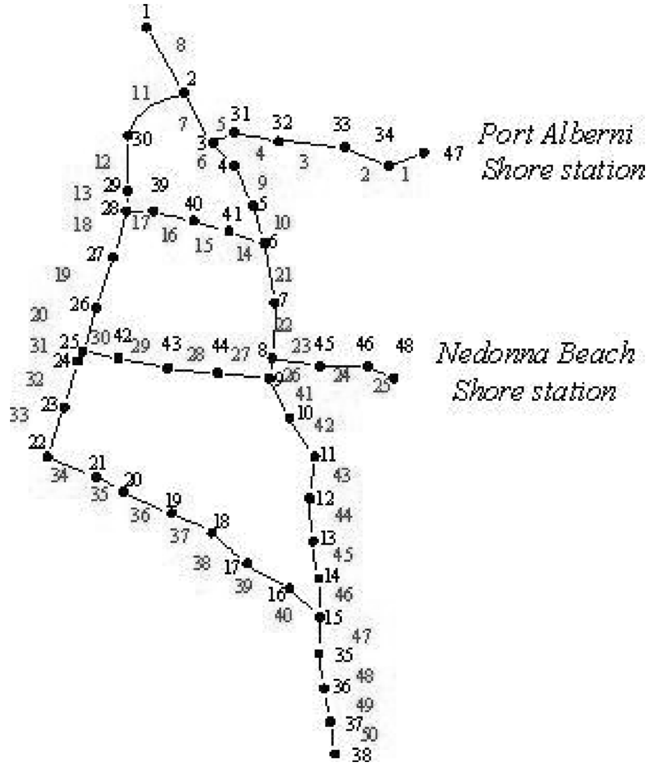

Fig. 6. System topology with node and link numbers.

voltage drops. Fig. 6 shows the system topology with node and link numbers.

1) Generalization: For a system with a meshed structure, each branch corresponds to an unknown current. A fault from a line to ground is also modeled as a branch. For a system condition under which no external load is connected, the fault current is known and it is the sum of all input currents.

For a system with multiple sources, multiple equations can be written based on the circuit parameters and the current flowing through each path. For a Y-shape branch, there are a total of three currents, but one of them can be expressed as the sum or difference of the other two. When there is no external load, 1/3 of the branch currents can be expressed in terms of a known current and another unknown current(s). This procedure reduces the total number of unknowns in the system to 2/3 of the number of unknown currents plus the addition of the fault resistance and faulted section cable resistance. For a fault on a system with multiple sources to be determined, the total number of paths from the sources to the fault should be larger than or equal to the total number of unknowns for any given fault in the system.

Based on the result from the previous paragraph, the total number of unknowns for the NEPTUNE system is 7, i.e., fault resistance, faulted cable resistance fraction n, and the number of unknown currents on different paths. There are two sources and the number of available paths from the two sources to anywhere in the system is larger than 7. Therefore, all fault locations on the NEPTUNE system are well specified. The equations for the paths can be written in the following general form (2):

$$V_{SSi} = \sum_{p_{ij}} (I_{p_{ij}} R_{p_{ij}} + V_{D_{p_{ij}}}) + \frac{1}{2} V_{D\_faulted\_link} + I_{faulted\_link} n R_{faulted\_link} + I_f R_f \quad (2)$$

where

V_{SSi}	voltage outputs of Shore Station i, i = 1, 2;
P_{ij}	jth path from shore station i to the fault, i = 1, 2;
I_{pij}	currents on links of the path;
R_{pij}	cable resistance of the links of the path;
V_{Dpij}	voltage drop across links of the path
$V_{D\_faulted\_link}$	voltage drop across the faulted link;
I_{fault_link}	current on the faulted link;
n	per unit distance of the faulted link;
R_{fault_link}	cable resistance of the faulted link;
I_f	fault current;
R_f	fault resistance.

In the proposed formulation, the current direction is assumed to be from the shore station toward the fault. The equations needed are chosen based on the *shortest distance paths* from each shore station to the faulted link. Current directions on the shortest path will apply to the next paths identified for loop analysis. Since the cable resistance is associated with an error, the shortest cable length would introduce the smallest error. In PMACS, the paths are identified automatically by shortest-path search.

2) System Modeling for NEPTUNE: Now suppose a backbone cable fault is present on cable link 9 between nodes 4 and 5. The voltage and current measurements from both shore stations are given. Since the topology is known, the loop equation from each shore station to the fault can be written. For the loop equations, path P_{11} includes cable links 1, 2, 3, 4, 5, and 6 and path P_{12} includes cable links 25, 24, 23, 22, 21, and 10. Each equation is nonlinear with unknown currents as in (3) and (4). The nonlinearity is due to the nature of the Zener diodes in the system

$$\begin{aligned} V_{SS1} = {} & I_1R_1 + V_{D1} + I_2R_2 + V_{D2} + I_3R_3 + V_{D3} \\ & + I_4R_4 + V_{D4} + I_5R_5 + V_{D5} + I_6R_6 + V_{D6} \\ & + \frac{1}{2}V_{D9} + I_{9'}nR_9 + I_9R_f \qquad (3) \\ V_{SS2} = {} & I_{25}R_{25} + V_{D25} + I_{24}R_{24} + V_{D24} + I_{23}R_{23} + V_{D23} \\ & + I_{22}R_{22} + V_{D22} + I_{21}R_{21} + V_{D21} \\ & + I_{10}R_{10} + V_{D10} + \frac{1}{2}V_{D9} + I_{9''}mR_9 + I_9R_f \qquad (4) \end{aligned}$$

where

V_{SSi}	voltage outputs of Shore Station i, i = 1, 2;
I_k	current on link k, k = 1 . . . 50;
V_{Dk}	voltage drop across link k, k = 1 . . . 50;
$I_{9'}$	current on link 9 from Node 4 to fault;
$I_{9''}$	current on link 9 from Node 5 to fault;
m, n	per unit distance of Link 9;
R_f	fault resistance.

The faulted link can be expressed in per-unit length such that:

$$nR_{fault\_link} + mR_{fault\_link} = R_{fault\_link}. \tag{5}$$

Additional nonlinear equations need to be written by loop analysis from the shore stations to the fault via the *next shortest paths* from shore stations 1 and 2, respectively, as shown in (6) and (7)

$$\begin{aligned} V_{SS1} &\\ = I_1R_1 &+ V_{D1} + I_2R_2 + V_{D2} + I_3R_3 + V_{D3}\\ &+ I_4R_4 + V_{D4} + I_5R_5 + V_{D5} + I_7R_7 + V_{D7}\\ &+ I_{11}R_{11} + V_{D11} + I_{12}R_{12} + V_{D12} + I_{13}R_{13} + V_{D13}\\ &+ I_{17}R_{17} + V_{D17} + I_{16}R_{16} + V_{D16} + I_{15}R_{15} + V_{D15}\\ &+ I_{14}R_{14} + V_{D14} + +I_{10}R_{10} + V_{D10}\\ &+ \frac{1}{2}V_{D9} + I_{9''}mR_9 + I_9R_f \end{aligned} \tag{6}$$

$$\begin{aligned} V_{SS2} &\\ = I_{25}R_{25} &+ V_{D25} + I_{24}R_{24} + V_{D24} + I_{23}R_{23} + V_{D23}\\ &+ I_{22}R_{22} + V_{D22} + I_{22}R_{22} + V_{D22} + I_{21}R_{21} + V_{D21}\\ &-(I_{14}R_{14} + V_{D14}) - (I_{15}R_{15} + V_{D15}) - (I_{16}R_{16} + V_{D16})\\ &-(I_{17}R_{17} + V_{D17}) - (I_{13}R_{13} + V_{D13}) - (I_{12}R_{12} + V_{D12})\\ &-(I_{11}R_{11} + V_{D11}) - (I_7R_7 + V_{D7})\\ &+ I_6R_6 + V_{D6} + \frac{1}{2}V_{D9} + I_{9'}nR_9 + I_9R_f. \end{aligned} \tag{7}$$

Note that all link currents are unknowns; however, since there is no load during fault location, shore station currents are feeding the fault point. Therefore

$$I_{SS1} + I_{SS2} = I_9 \tag{8}$$

where

I_{SSi} current outputs of Shore Station i, i = 1, 2.

From the topology of the system, it can be seen that

$$I_{SS1} = I_1 = I_2 = I_3 = I_4 = I_5 \tag{9}$$

$$I_{SS2} = I_{23} = I_{24} = I_{25} \tag{10}$$

$$I_7 = I_{11} = I_{12} = I_{13} = I_{SS1} - I_6 \tag{11}$$

$$I_{14} = I_{15} = I_{16} = I_{17} = I_{9''} - I_{21}. \tag{12}$$

Similarly, the current of any other link can be written as an expression of the known currents I_{SS1}, I_{SS2}, and some unknown current(s). Substitute (9)–(12) into (3), (4), (6), and (7), the number of unknowns in the equations is reduced. The number of nonlinear equations needed to solve a fault on a specific link is different for each link.

The number of nonlinear equations should be 1 less than the number of unknowns since there is an unknown fault resistance. However, with the addition of (5), there is an equal number of equations and hence the solution can be found by numerical techniques. MATLAB is used to solve the nonlinear equations for the values of m and n.

D. Worst-Case Analysis

When taking the voltage and current measurements at the two shore stations, each of them is subject to error. This error affects the result of the estimated resistance and hence the estimated fault location. To reduce the error effect, multiple independent measurements should be taken at shore stations.

Assume that the line resistance is $1\ \Omega/\mathrm{km}$. Since the goal is to locate the fault to within $\pm 1\ \mathrm{km}$, the error in terms of resistance should be within $\pm 1\ \Omega$. If the error in resistance for the worst case can be contained within $\pm 1\ \Omega$, the error in fault distance would be smaller than $\pm 1\ \mathrm{km}$ for any other cases. In this study, a worst case analysis is conducted to determine the maximum allowable voltage and current measurement errors.

Note that the *worst case* resistance as a random variable and its *variances* are given by

$$\frac{V_1}{I_1} = R_{\max}$$

$$\sigma^2_{R_{\max}} = \sigma^2_{V_1}\left(\frac{\partial R}{\partial V_1}\right)^2 + \sigma^2_{I_1}\left(\frac{\partial R}{\partial I_1}\right)^2 + 2\sigma_{V_1I_1}\left(\frac{\partial R}{\partial V_1}\right)\left(\frac{\partial R}{\partial I_1}\right)$$

where

$$\left(\frac{\partial R}{\partial V_1}\right) = \frac{1}{I_1}$$

$$\left(\frac{\partial R}{\partial I_1}\right) = -\frac{V_1}{I_1^2}$$

$$\sigma^2_{R_{\max}} = \sigma^2_{V_1}\left(\frac{1}{I_1}\right)^2 + \sigma^2_{I_1}\left(-\frac{V_1}{I_1^2}\right)^2 + 2\sigma_{V_1I_1}\left(\frac{1}{I_1}\right)\left(-\frac{V_1}{I_1^2}\right)$$

$$\sigma^2_{R_{\max}} = \frac{\sigma^2_{V_1}}{I_1^2} + \frac{\sigma^2_{I_1}V_1^2}{I_1^4} - \frac{2\sigma_{V_1I_1}V_1}{I_1^3}.$$

Now assume a *non-worst case* $\mathrm{R} < \mathrm{R}_{\max}$, V_1 remains the same since it is the shore station output voltage and hence $\mathrm{I}_1' > \mathrm{I}_1$

$$\frac{V_1}{I_1'} = R$$

$$\sigma^2_R = \sigma^2_{V_1}\left(\frac{1}{I_1'}\right)^2 + \sigma^2_{I_1}\left(-\frac{V_1}{(I_1')^2}\right)^2 + 2\sigma_{V_1I_1}\left(\frac{1}{I_1'}\right)\left(-\frac{V_1}{(I_1')^2}\right)$$

$$\Rightarrow \sigma^2_R < \sigma^2_{R_{\max}}.$$

Using the values for the NEPTUNE system, it is found that the worst case is a fault on link 50 since the cable resistance and voltage drops are both the largest among all fault scenarios. This analysis suggests that if the algorithm can locate a fault on link 50 within $\pm 1\ \mathrm{km}$, it should locate any other fault on the NEPTUNE system within better than $\pm 1\ \mathrm{km}$.

E. Voltage Level Requirement

As mentioned, when a fault occurs, the system shuts down and then restarts with a positive voltage. The Zener diodes have a knee current of about 150 mA. In this region, the voltage drop is proportional to the current (and hence is not constant). Due to the nature of the system, some currents on the branches might be very small. Since there is no communication during the fault location mode, the currents on the branches are unknown.

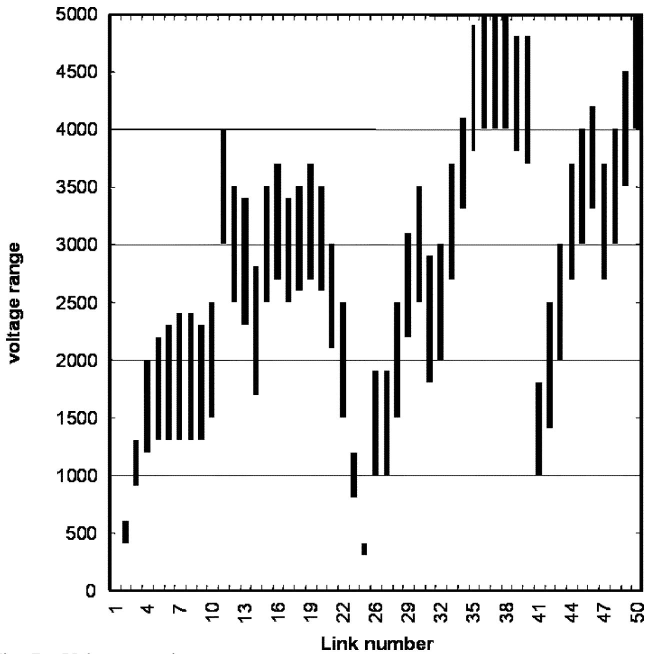

Fig. 7. Voltage requirements.

Therefore, voltage outputs at the shore stations need to reach a sufficient level to ensure that all currents on the branches are large enough so that the Zener diodes will have constant voltage drops. The shore station voltage requirements vary when a fault is located on different links. For a fault on a specific link, there is a required minimum voltage to locate the fault to within 1 km. There is also a maximum voltage level for each specific scenario since the maximum current allowed on a backbone cable should not exceed 10 A. If the voltage at the shore station is higher than the maximum allowable level, the backbone current exceeds 10 A somewhere in the system.

During restarting, sometimes voltage and current measurements for fault location are taken before the system goes back to normal operation. In this case, the faulted link is not known at the point when measurements are taken. Therefore, the voltage levels to apply at the shore stations cannot be determined. Instead, current outputs at the shore stations are raised until the sum of the two currents is close to 10 A. This ensures that Zener diodes are operating in the saturated region, and the constraint of 10 A is not exceeded.

If the system operator decides to go back to normal operation without taking fault measurements and come back for the measurements at a later time, the faulted link can be identified before the measurements are taken. In this case, the system can apply a voltage level that would guarantee the sufficient level of current in the branches without violating the current limit. Fig. 7. shows the minimum and maximum allowable voltage levels necessary to resolve a fault location on a given link to the desired accuracy.

Notice that link 1 and link 25 are connected to the shore stations. If the fault is located close to the shore station, even a small voltage might result in a high current. Since the true fault location is not known, the maximum voltage level can not be used in order to avoid a current that exceeds 10 A. Instead, the voltage at the shore stations is increased until the current reaches 5 A. The corresponding voltage and current measurements are then used to perform the fault location.

TABLE I
FAULT LOCATION RESULTS

Faulted Link	Faulted Location	Fault Resistance	Estimated Fault Location
9	20km from Node 4	2Ω	19.5km from Node 4
12	40km from Node 30	1Ω	39.7km from Node 30
16	25km from Node 40	2Ω	24.2km from Node 40
22	71km from Node 7	1Ω	71.6km from Node 7
28	10km from Node 44	1Ω	10.8km from Node 44
35	40km from Node 21	3Ω	38.6km from Node 21
44	20km from Node 12	3Ω	20.8km from Node 12
50	50.8km from Node 37	0Ω	49.9km from Node 37

F. Simulation Results for the NEPTUNE System

The first step to estimate the fault location for the NEPTUNE power system is to formulate the set of nonlinear equations similar to (3) and (4) for the proposed topology shown in Fig. 6. Port Alberni is Shore Station 1, and Nedonna Beach is Shore Station 2. For a given fault, the fault location algorithm constructs the nonlinear equations based on the discussion in Section III-C. The faulted link can be identified by the algorithm described in [7]. Although the constant voltage drops on the cable sections are not shown on the figure, their values are taken into account when formulating the equations. The number of equations required to solve for the fault location depends on the specific faulted link.

Table I shows some results of simulated cable faults on different links with different fault resistances. A normally distributed random error of zero mean and 0.01% standard deviation is added to the voltage and current shore station measurements. The calculation has been performed 30 times simulating 30 sets of independent measurements.

Assume that a fault is presented at the far end of link 50 to represent the worst case scenario. When both shore stations have a voltage output of 4300 V, I_1 is 1.51 A and I_2 is 4.33 A. When solving the nonlinear equations, it yields an average solution of $n = 0.9958$ and $m = 0.0042$. Since the line segment is 215 km long, the error in estimating the fault location is m times 215 or 0.9 km. Therefore, it shows that 4300 V from both shore stations would be a sufficient voltage level to handle the worst case. For faults in different locations in the system, the voltage level does not exceed 4300 V.

As shown in Table I, the estimated fault location is very close to the actual location in most cases. The only case where the algorithm does not meet the 1 km requirement is the cable fault on Link 35, with an error of 1.4 km. This could be due to the fact that Link 35 is very far from both shore stations yielding large errors in measurements and the fault resistance is larger than other cases.

G. Implementation of Fault Location Method

The implementation of Fault Location method is discussed in detail in this section, Section III-G. The software environment

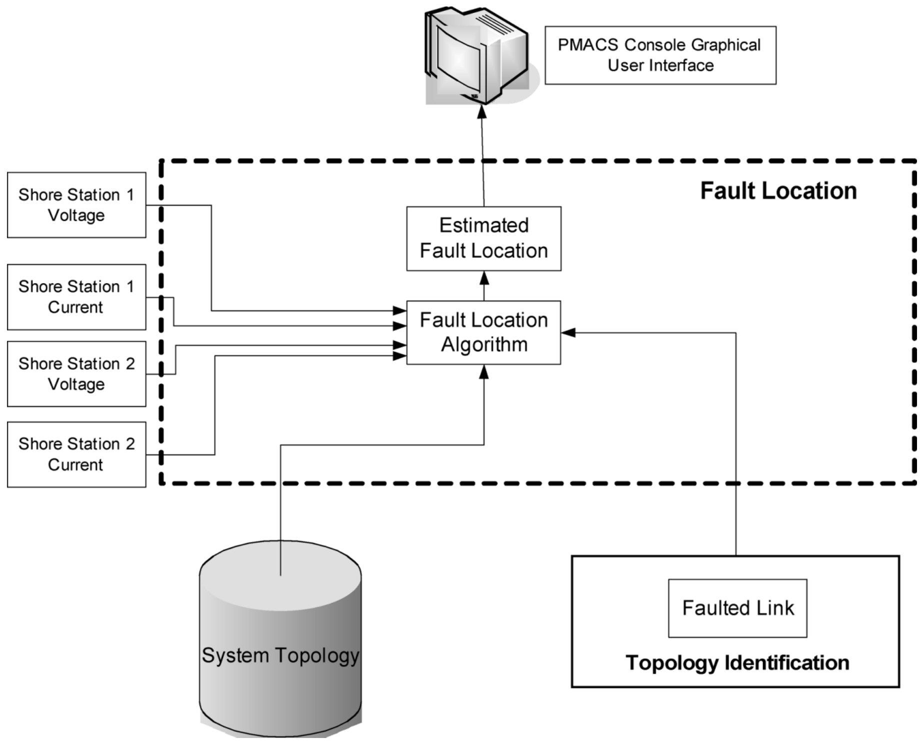

Fig. 8. Fault location implementation for PMACS.

is presented first. Then, the design of PMACS system, which is responsible for data acquisition and user interface for Fault Location, is summarized. As shown in Fig. 8, the implementation of the proposed fault location algorithm for PMACS requires the following information: 1) faulted link identity; 2) real-time voltage and current measurements from both shore stations; and 3) system topology. The faulted link will be identified by the Topology Identification module of PMACS. PMACS will set the voltage levels for the shore stations and measure the current outputs. The topology is stored in a database.

In this study, a software module has been developed for the fault location function. Fig. 9 shows the PMACS user interface for the Fault Location module for NEPTUNE. Currently, the shore station measurements are generated by simulated data. The measurements are processed by the fault location algorithm software. The estimated fault location is displayed through the user interface.

The results reported in the previous section of this paper are simulated by computer software. As a test bed of NEPTUNE, the Monterey Accelerated Research System (MARS) in Monterey, CA, will provide field test results.

The MARS project, headed by Monterey Bay Aquarium Research Institute (MBARI), is near completion at the time of this writing and is scheduled for late 2006 installation. The power system is described in [16]. The MARS system has one Shore Station and one Science Node. There are sea grounds at each end of the system, i.e., the Shore Station and the Science Node. The cable is standard telecommunications cable (Alcatel OALC4, 17 mm diameter core, 1.6 Ω/km) and the backbone communications technology is 100 Mb/s Ethernet. The communication protocol is TCP/IP. The primary communications between the Node Controller and the PMACS uses the 100BaseT Ethernet provided by the Data Communications Subsystem (DCS). There is a secondary serial RS-232 communications channel for use during operations, in the case of a loss of the primary communications system or for maintenance or troubleshooting.

The Shore Station contains a high-voltage power supply from Universal Voltronics (± 15 kV DC, 1.111 A) with adjustable polarity, shore ground, the Power Supply Controller (PSC), and the PMACS server computer. The server is on the local area network, synchronized by GPS.

The implementation of the Neptune PMACS is illustrated in Fig. 10. The same architecture is used by MARS. PMACS is constructed with a three-layer client-server architecture. At the lowest layer are the Node Power Controller (NPC) and Power Supply Controller (PSC), in the middle is the PMACS Server, and on top are the PMACS Console and Clients. The NPC is consisted of one CPU board and four analog/digital I/O boards. The PMACS Server is a HP Intel-based server with RedHat Linux. The Console and Client software is developed using MS Visual Basic.NET. The Console contains the main user interface for the operator to interact with the actual system, and also provides analytical tools such as the Fault Location module. There may be multiple Clients but, at any given time, there must be one Console in communication with the Server. The communications between the Console/Client and the Server is using Simple Object Access Protocol (SOAP).

The PMACS Server and NPC are able to acquire accurate absolute time-of-day from the DCS. Network Time Protocol (NTP) is used for time-of-day, with an accuracy of approximately 10 msc. The NPC, PMACS Server, and PMACS Console are on the same NTP Server to make sure they are all synchronized.

Although the MARS system is much simpler than the planned NEPTUNE system, with only one Shore Station and one Sci-

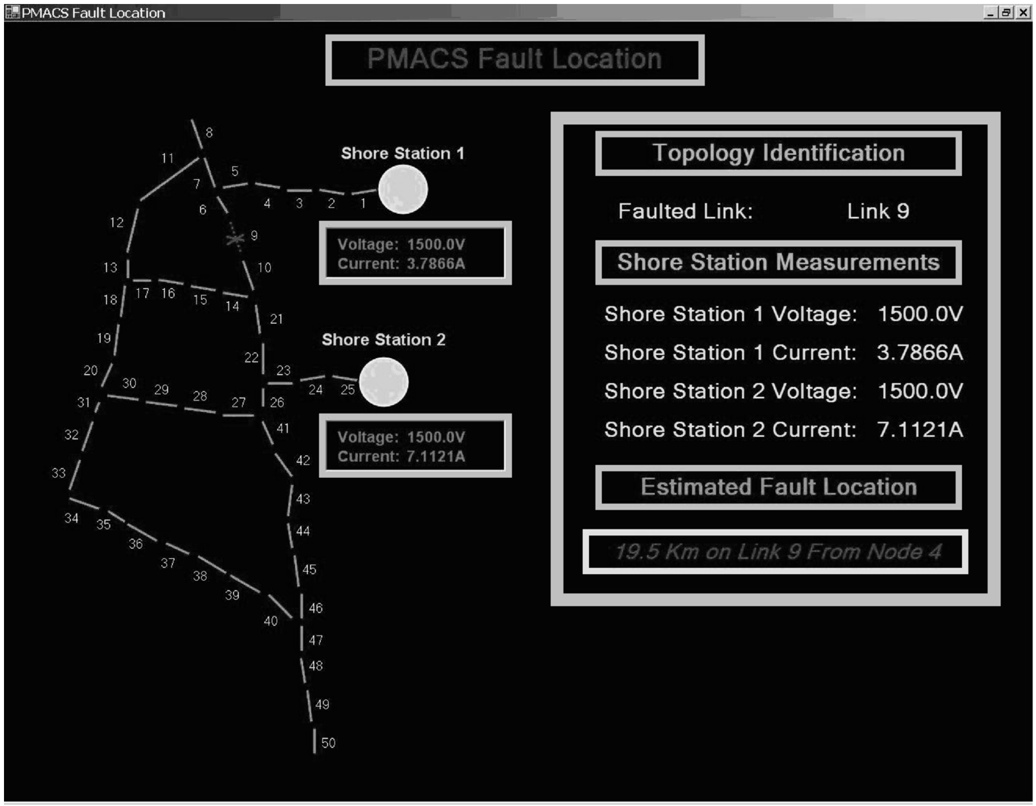

Fig. 9. PMACS user interface for fault location.

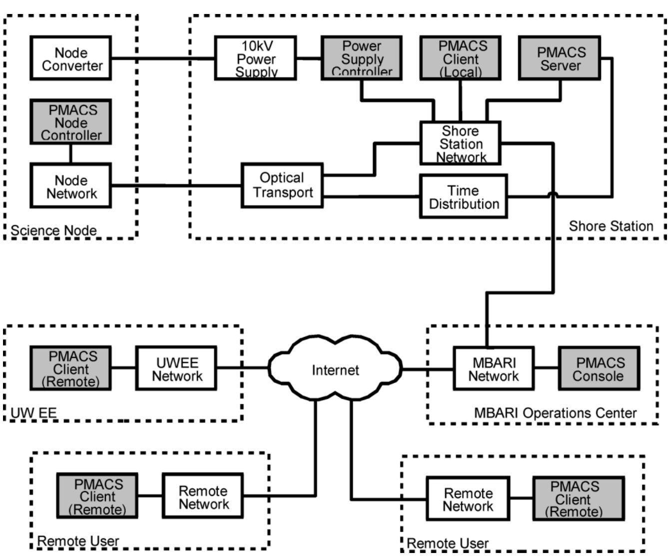

Fig. 10. MARS PMACS.

ence Node, the PMACS architecture and operation philosophy is the same. Neptune and MARS have the same Fault Location module that use the method described in this paper to estimate the location of a fault on the backbone cable. The communications protocols, devices, and PMACS hardware are the same for both systems. Real-time voltage and current measurements are taken at the Shore Station by the PSC. The PMACS Server will send the data to the PMACS Console for the Fault Location module to perform the calculation.

TABLE II
FAULT LOCATION LAB TEST RESULTS.

Input Voltage	Measured Voltage	Measured Current	Estimated Resistance	Actual Resistance
375V	375.53V	12.48A	29.38Ω	29.90Ω
48V	47.44V	1.62A	29.27Ω	29.90Ω
375V	375.62V	24.18A	15.55Ω	15.43Ω
48V	47.46V	3.17A	14.98Ω	15.43Ω

H. Lab Test Results

A lab test has been performed to verify the proposed fault location algorithm using the MARS PMACS software and hardware. Instead of the actual high voltage power supply, a low voltage power supply is used in the lab environment. Instead of the Power Supply Controller, a Node Power Controller with similar functionality and accuracy is used. Resistors are connected in series to simulate the backbone cable. The Node Power Controller measures the input voltage and current. These measurements are acquired by PMACS and processed by the Fault Location module to obtain the (estimated) resistance. The results are shown on the PMACS Console.

The test is conducted at two different voltage levels: 375 V and 48 V. Two different fault scenarios are tested by using 2 different values of resistances: 29.9 Ω and 15.43 Ω. Depending on the type of cable being used in Neptune and MARS, these values represent the location of the backbone cable fault from the Shore Station. Measurements are taken over a 10-s time span which includes ten samples. The lab test results are shown in Table II.

The results show that the estimated resistances are within 1 Ω of the actual resistances. These results indicate that the estimated fault location from the proposed algorithm is within 1 km of the actual fault location.

IV. Applications

Underwater power systems require a highly accurate fault location technique due to the high cost of repair. The algorithm described in this paper does not require extensive monitoring devices to be installed at various locations on the system. Similar methods may be applied to some terrestrial power systems such as underground distribution systems. Underground distribution systems need to be highly reliable since they are usually located in urban areas with a higher density of load. The difficulty of locating or repairing an underground cable fault is significantly higher than overhead lines. The method described in this paper is a good addition to the existing fault location techniques such as TDR.

The Electric Power Research Institute (EPRI) also has a project that uses a similar concept [17] to locate cable faults for rural distribution systems. The research is based on the method described in [18] which uses a Feeder Monitoring System (FMS) to record the voltages and currents on a feeder. The method described in [18] uses the recorded fault current to compare with a default value stored in a database to estimate the location of a fault based on the feeder impedance.

Impedance-based fault location techniques are used in power systems. The most common impedance-based methods are one-end and two-end methods [19]. The applications are for a single line of AC systems. The method proposed in this paper uses a similar method which is designed for a networked DC system.

V. Conclusion

The algorithm developed in this research is a full scale version of the resistance estimation method that is used in point-to-point underwater applications. It has the ability to locate a cable fault in a meshed configuration and does not have the limitation of cable length as it does for the TDR method. The same algorithm may also be applied in underground cable systems or HVDC systems.

Besides the MARS test bed, the next large test bed for regional cabled ocean observatories will be the northern portion of NEPTUNE, presently under construction by NEPTUNE Canada [20]. It will be a 4-node, 800-km loop terminated at Port Alberni. It will use a hybrid series-parallel power system. The series portion will power optical repeaters and the optical supervisory system that will, among other functions, control the BU breakers.

Appendix

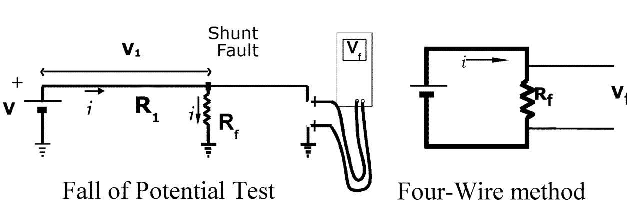

Fig. 11. Fall-of-potential test and four-wire method.

The fall-of-potential test is also referred to as the "three point method". The test is typically used to determine the ground resistance of the earth [21]. The goal of the fall-of-potential test in this study is to investigate the nature of the shunt fault [15]. This test is performed by applying a voltage at one end of a faulted cable and measuring the voltage drop across the shunt fault at the other end of the cable. When conducting the fall-of-potential test, the first step is to open the measuring end then power the sending end through the fault as shown in Fig. 11. A voltmeter is connected to the measuring end to measure the voltage drop across the shunt fault, V_f. The method is equivalent to the four-wire method also shown in Fig. 11, with the ocean replacing the return wires to the two ends. With no current going to the voltmeter, it reads the fault voltage directly. The fault current is measured at the sending end. The fault resistance can then be calculated directly. (Note that the information available can also be used to find the resistance of the cable between the sending end and the fault. This value is ordinarily sufficient to locate the fault in a point-to-point system.)

Acknowledgment

The authors would like to thank C. Siani, T. McGinnis, M. Kenny, P. Pilgrim, P. Lancaster, and W. Beckman for their help in this research.

References

[1] J. Delaney, G. R. Heath, A. Chave, H. Kirkham, B. Howe, W. Wilcock, P. Beauchamp, and A. Maffei, "NEPTUNE real-time, long-term ocean and earth studies at the scale of a tectonic plate," in *Proc. Oceans 2001, MTS/IEEE Conf. and Exhib.*, 2001, vol. 3, pp. 1366–1373.

[2] B. Howe, H. Kirkham, and V. Vorperian, "Power system considerations for undersea observatories," *IEEE J. Ocean. Eng.*, vol. 27, no. 2, pp. 267–274, Apr. 2002.

[3] B. Howe, H. Kirkham, V. Vorperian, and P. Bowerman, "The design of the NEPTUNE power system," in *Proc. Oceans 2001, MTS/IEEE Conf. and Exhib.*, 2001, vol. 3, pp. 1374–1380.

[4] K. Schneider, C. C. Liu, T. McGinnis, B. Howe, and H. Kirkham, "Real-time control and protection of the NEPTUNE power system," in *Proc. Oceans 2002, MTS/IEEE Conf. and Exhib.*, 2002, vol. 2, pp. 1799–1805.

[5] P. Fairley, "NEPTUNE rising," *IEEE Spectrum*, vol. 42, no. 11, pp. 38–45, Nov. 2005.

[6] M. A. El-Sharkawi, A. Upadhye, S. Lu, H. Kirkham, B. Howe, T. McGinnis, and P. Lancaster, "North East Pacific Time-integrated Undersea Networked Experiments (NEPTUNE): Cable switching and protection," *IEEE J. Oceans Eng.*, vol. 30, no. 1, pp. 232–220, Jan. 2005.

[7] K. Schneider, C. C. Liu, and B. Howe, "Topology error identification for the NEPTUNE power system," *IEEE Trans. Power Syst.*, vol. 20, no. 3, pp. 1224–1232, Aug. 2005.

[8] K. Schneider, C. C. Liu, B. Howe, and H. Kirkham, "State estimation for the NEPTUNE power system," in *Proc. Transmission and Distribution Conf.*, Sep. 2003, vol. 2, pp. 748–754.

[9] M. Kezunovic, P. Spasojevic, C. W. Fromen, and D. R. Sevcik, "An expert system for transmission substation event analysis," *IEEE Trans. Power Del.*, vol. 8, pp. 1942–1949, Oct. 1993.

[10] T. Baldwin, F. Renovich, Jr., L. F. Saunders, and D. Lubkeman, "Fault locating in ungrounded and high-resistance grounded systems," *IEEE Trans. Ind. Appl.*, vol. 37, no. 4, pp. 1152–1159, Jul.-Aug. 2001.

[11] J. Jung, C. C. Liu, M. Hong, M. Gallanti, and G. Tornielli, "Multiple hypotheses and their credibility in on-line fault diagnosis," *IEEE Trans. Power Del.*, vol. 16, pp. 225–230, Apr. 2001.

[12] J. A. Jiang, J. Z. Yang, Y. H. Lin, C. W. Liu, and J. C. Ma, "An adaptive PMU based fault detection/location technique for transmission lines. Part I: Theory and algorithms," *IEEE Trans. Power Del.*, vol. 15, no. 2, pp. 486–493, Apr. 2000.

[13] P. Menconi and D. J. Liparoto, "Tracking and fault location in undersea cables," in *Proc. Oceans 1992, Mastering the Oceans Through Technology*, 1992, vol. 2, pp. 678–683.

[14] S. Navaneethan, J. J. Soraghan, W. H. Siew, F. McPherson, and P. F. Gale, "Automatic fault location for underground low voltage distribution networks," *IEEE Trans. Power Del.*, vol. 16, no. 2, pp. 346–351, Apr. 2001.

[15] P. Pilgrim, "Analysis and Location of Shunt Faults," Intern. Rep. 360networks, 2000.

[16] B. M. Howe, T. Chan, M. E. Sharkawi, M. Kenney, S. Kolve, C. C. Liu, S. Lu, T. McGinnis, K. Schneider, C. Siani, H. Kirkham, V. Vorperian, and P. Lancaster, "Power system for the MARS ocean cabled observatory," in *Proc. Scientific Submarine Cable 2006 Conf.*, Dublin Castle, Dublin, Ireland, Feb. 2006.

[17] Project Set 128B, P128.002 Electric Power Research Institute, Palo Alto, CA [Online]. Available: http://www.epri.com/portfolio/product.aspx?id=1490&area=38&type=10

[18] G. C. Lampley, "Fault detection and location on electrical distribution system case study," in *Proc. Rural Electrical Power Conf.*, May 2002, p. B1-B1-5.

[19] K. Zimmerman and D. Costello, "Impedance-based fault location experience," in *Proc. 58th Annu. Conf. Protective Relay Engineers*, Apr. 2005, pp. 211–226.

[20] P. Phibbs and S. Lentz, "Selection of the technical design of the world's first regional cabled observatory – NEPTUNE stage 1 (NEPTUNE Canada)," in *Proc. Scientific Submarine Cable 2006 Conf.*, Dublin Castle, Dublin, Ireland, Feb. 2006.

[21] *IEEE Guide for Measuring Ground Resistivity, Ground Impedance, Ground Surface Potentials of a Ground System*, , Mar. 1983, IEEE Standard 81-1983.

Ting Chan (S'99) received the B.S. and M.S. degrees in electrical engineering in 1999 and 2001, respectively, from the University of Washington, Seattle, where he is currently pursuing the Ph.D. degree in electrical engineering. His main area of research is the NEPTUNE power system.

He received the Grainger Graduate Fellowship from the University of Washington in 2002.

Chen-Ching Liu (F'94) received the B.S. and M.S. degrees in electrical engineering from National Taiwan University, Taipei, Taiwan, R.O.C., and the Ph.D. degree from the University of California, Berkeley.

He is currently Palmer Chair Professor of Electrical and Computer Engineering at Iowa State University, Ames. During 1983–2005, he was a Professor of Electrical Engineering at the University of Washington, Seattle, where he also served as an Associate Dean of Engineering during 2000–2005.

Dr. Liu received the 2004 IEEE Power Engineering Society's (PES) Outstanding Power Engineering Educator Award. He is Chairing the IEEE PES Technical Committee on Power System Analysis, Computing and Economics.

Bruce Howe (M'02) received the B.S. degree in mechanical engineering and the M.S. degree in engineering science in 1978, both from Stanford University, Stanford, CA, and the Ph.D. degree in oceanography in 1986 from the Scripps Institution of Oceanography, University of California, San Diego.

While at Stanford, he developed laser Doppler velocimetry (LDV) instrumentation for air-sea interaction experiments. From 1979 to 1981, he was a Research Associate at the Institute Für Hydromechanik, Universität Karlsruhre, Karlsruhre, Germany, working on LDVs for use in the atmospheric boundary layer. While at Scripps and since then, he has worked on ocean acoustic tomography, most recently on the Acoustic Thermometry of Ocean Climate (ATOC) project. He is presently a Principal Oceanographer at the Applied Physics Laboratory, a Research Associate Professor in the School of Oceanography, and an Adjunct Research Associate Professor in Electrical Engineering, all at the University of Washington. His current interests include cabled seafloor observatories, specifically the NEPTUNE project focused on the Juan de Fuca Plate, and integrating acoustics systems into ocean observatories on all scales, from meters to basin-scale

Harold Kirkham (F'04) received the B.S. degree in 1966 and the M.S. degree in 1967, both from the University of Aston, Birmingham, U.K., and the Ph.D. degree from Drexel University, Philadelphia, PA, in 1973.

He was with American Electric Power at their UHV station in Indiana. He has been at the Jet Propulsion Laboratory (JPL), Pasadena, CA, since 1979, in a variety of positions. For several years, he was Manager of the NEPTUNE power project. He is presently a Principal in the Office of Mission Assurance. His research interests include both power and measurements.

Dr. Kirkham is a Past-Chair of the IEEE Power Engineering Society's Instrumentation and Measurements Committee.